

Detecting crystal symmetry fractionalization from the ground state: Application to \mathbb{Z}_2 spin liquids on the kagome lattice

Yang Qi

*Institute for Advanced Study, Tsinghua University, Beijing 100084, China and
Perimeter Institute for Theoretical Physics, Waterloo, ON N2L 2Y5, Canada*

Liang Fu

Department of Physics, Massachusetts Institute of Technology, Cambridge, MA 02139, USA

In quantum spin liquid states, the fractionalized spinon excitations can carry fractional crystal symmetry quantum numbers, and this symmetry fractionalization distinguishes different symmetry-enriched spin liquid states with identical intrinsic topological order. In this work we propose a simple way to detect signatures of such crystal symmetry fractionalizations from the crystal symmetry representations of the ground state wave function. We demonstrate our method on projected \mathbb{Z}_2 spin liquid wave functions on the kagome lattice, and show that it can be used to classify generic wave functions. Particularly our method can be used to distinguish several proposed candidates of \mathbb{Z}_2 spin liquid states on the kagome lattice.

PACS numbers: 75.10.Kt, 05.30.Pr, 61.50.Ah

It is well known that anyons in topologically ordered phases can carry symmetry quantum numbers that are quantized to fractional values. In the celebrated example of fractional quantum Hall states, Laughlin quasiparticles carry fractional charge—the quantum number of the $U(1)$ symmetry [1]. In recent years, great progress has been made in understanding the interplay between symmetry and fractionalization in other topologically ordered states. In particular, topological spin liquids exhibit a more subtle kind of symmetry fractionalization, associated with the crystal symmetry of the underlying lattice instead of internal symmetries [2–4]. While some aspects of it have been studied for quite a while, crystal symmetry fractionalization has now received renewed attention, due to an increased interest in the role of crystal symmetry in topological phases of matter. This topic is also becoming timely in view of strong numerical evidence for spin liquids on kagome lattice found in the last few years [5–9]. In order to fully pin down the topological nature of the numerically found spin liquid liquid, the complete pattern of crystal symmetry fractionalization needs to be determined.

In this work, we offer a new perspective on crystal symmetry fractionalization in \mathbb{Z}_2 spin liquids. We find that the nontrivial way that crystal symmetry acts on an individual anyon is directly related to the symmetry representation of the topologically ordered ground states, as labeled by the crystal momentum and parity of many-body wave functions. Given that states with different symmetry labels cannot be adiabatically connected, our finding immediately makes it clear that the classification of spin liquids is refined and enriched by taking into account crystal symmetries [10]. Our theoretical result also provides a straightforward method to classify and detect different spin liquids in numerical studies. As a concrete example, we demonstrate that our method can be used to

easily distinguish various \mathbb{Z}_2 spin liquids on the kagome lattice [11–13].

We begin by briefly reviewing what is known about crystal symmetry fractionalization in \mathbb{Z}_2 spin liquids, and setting up the terminology for our work. A \mathbb{Z}_2 spin liquid [14, 15] supports three types of anyon excitations: bosonic spinons, fermionic spinons, and visons. As a defining property of topological excitations, anyons of each type can only be created in pairs. This property makes symmetry fractionalization possible. This can be understood by considering a many-body excited state containing two identical anyons that are spatially separated [3, 16]. Intuitively speaking, the action of symmetry on this excited state can then be factorized into a product of two independent symmetry actions on the anyons. While the action on a physical state is necessarily described by a *linear* representation of the symmetry group denoted by G , the action on a single anyon is now allowed to form a *projective* representation \tilde{G} , such that the tensor product $\tilde{G} \otimes \tilde{G}$ is a linear representation of G [17–20]. The projective representation \tilde{G} , which has a different group algebra than G , can be regarded as the “square root” of G . In this sense, symmetry action on anyons can be called “fractionalized.” Throughout this Rapid Communication, a tilde symbol ($\tilde{}$) placed over a symmetry operation means that it acts on an anyon; otherwise it acts on a physical wave function.

To sharpen the intuitive argument stated above and give a precise definition of symmetry fractionalization is a nontrivial task that requires great care. The main difficulty is that symmetry operations should in principle be performed on a single anyon, and yet any physical wave function necessarily contains an even number of them. (We note that crystal symmetry fractionalization may have implications for excitation spectra that can be detected [2, 21, 22].) To overcome this difficulty, we take a

different approach and give a precise and *operational* definition of crystal symmetry fractionalization by relating it to the *linear* symmetry representations of many-body wave functions.

Crystal symmetries of a given lattice form a space group G generated by translation, rotation and reflection. Any allowed projective representation of G , denoted by \tilde{G} , can be specified by its modified group algebra as compared to G [2, 4]. First, two commuting operations X and Y in G , $XY = YX$, can become anti-commuting in \tilde{G} , $\tilde{X}\tilde{Y} = -\tilde{Y}\tilde{X}$. This will be referred to as commutation relation fractionalization. Second, an identity of $X^n = 1$ in G can become $\tilde{X}^n = -1$ in \tilde{G} . This will be referred to as quantum number fractionalization.

As the main result of this work, we find that the symmetry representation of ground states is a diagnosis of crystal symmetry fractionalization in \mathbb{Z}_2 spin liquids. First, the commutation relation between a translation operation T_1 and another symmetry operation X , $\tilde{T}_1\tilde{X} = \pm\tilde{X}\tilde{T}_1$, can be determined from the difference between eigenvalues of X for ground states in *different* topological sectors on a torus geometry with an *odd* number of unit cells in the direction of T_1 . Second, for an order-two symmetry operation $X^2 = 1$, $\tilde{X}^2 = \pm 1$ can be determined from the parity eigenvalue of X acting on ground states on a torus with $4n + 2$ sites. We find it remarkable that the fractionalized symmetry property of anyons is simply and directly encoded in the symmetry of ground states. Some technical details of our derivation are available in the Supplemental Material [23].

Fractionalized commutation relation. In the presence of a fractionalization in the commutation relation between T_1 and another symmetry operation X , ground states in different topological sectors have different eigenvalues of X on a torus with odd number of unit cells in the T_1 direction [3]. To extract the fractionalization of different anyons, we find it crucial to choose a basis according to the anyon flux along the direction of T_1 .

On a torus, a gapped \mathbb{Z}_2 spin liquid has a fourfold ground state degeneracy, which is protected by its intrinsic topological order. A basis of these four ground states can be chosen such that each state carries a different anyon flux going through the torus in the direction of T_1 , which can be diagnosed by a Wilson loop operator in the direction of T_2 [15]. There are four types of such flux; each corresponds to one type of anyon excitations in the toric code topological order. Therefore the four ground states can be labeled as $|G_a\rangle$, where a denotes the type of anyon. In this paper we denote the four types of anyon excitations in the \mathbb{Z}_2 spin liquid state as $a = 1, b, f$, and v , standing for the trivial particle, the bosonic spinon, the fermionic spinon, and the vison, respectively.

Using this basis, the ratio between parity eigenvalues of two ground states can be calculated by considering the Berry phase picked up through the following operations

acting on $|G_1\rangle$,

$$X^{-1}(f^a)^{-1}Xf^a|G_1\rangle = e^{i\Delta\Phi}|G_1\rangle, \quad (1)$$

where f^a denotes the operation of moving one a anyon across the torus in the direction of T_1 and it maps $|G_1\rangle$ to $f^a|G_1\rangle = |G_a\rangle$ [24]. This Berry phase $\Delta\Phi$ can be obtained from the ground state X -symmetry representations as the following,

$$\begin{aligned} |G_1\rangle &\xrightarrow{f^a} |G_a\rangle \xrightarrow{X} \lambda_X^a |G_a\rangle \\ &\xrightarrow{(f^a)^{-1}} \lambda_X^a |G_1\rangle \xrightarrow{X^{-1}} \lambda_X^a (\lambda_X^1)^{-1} |G_1\rangle, \end{aligned} \quad (2)$$

where λ_X^a denotes the parity eigenvalue of X acting on $|G_a\rangle$: $X|G_a\rangle = \lambda_X^a |G_a\rangle$.

On the other hand, the same Berry phase can be obtained using the projective crystal symmetry representation of the a anyon. Starting from the ground state $|G_1\rangle$, the operation f^a creates two anyons locally and moves one across the torus along T_1 , which is equivalent to acting T_1 on one of the two anyons n_1 times, so the end state can be expressed as $a \otimes \tilde{T}_1^{n_1} a$, where \otimes denotes anyon fusion and n_1 is the number of unit cells in the direction of T_1 , which is an odd number according to our setup. Then X acts on both anyons and maps the state to $\tilde{X}a \otimes \tilde{X}\tilde{T}_1^{n_1} a$. The rest of the actions can be calculated similarly,

$$\begin{aligned} 1 &= a \otimes a \xrightarrow{f^a} a \otimes \tilde{T}_1^{n_1} a \xrightarrow{X} \tilde{X}a \otimes \tilde{X}\tilde{T}_1^{n_1} a \\ &\xrightarrow{(f^a)^{-1}} \tilde{X}a \otimes \tilde{T}_1^{-n_1} \tilde{X}\tilde{T}_1^{n_1} a \xrightarrow{X^{-1}} a \otimes \tilde{X}^{-1} \tilde{T}_1^{-n_1} \tilde{X}\tilde{T}_1^{n_1} a. \end{aligned}$$

Hence after the series of operations one anyon is changed into $\tilde{X}^{-1} \tilde{T}_1^{-n_1} \tilde{X} \tilde{T}_1^{n_1} a = (\tau_X^a)^{n_1} a$, where $\tau_X^a = \pm 1$ denotes the fractionalization of the commutation relation, $\tilde{T}_1 \tilde{X} a = \tau_X^a \tilde{X} \tilde{T}_1 a$. This can be simplified as τ_X^a because n_1 is odd and $(\tau_X^a)^2 = 1$. Comparing this result with Eq. (2) we obtain the following relation between commutation relation fractionalization and ground state parity eigenvalues,

$$\tau_X^a = \lambda_X^a / \lambda_X^1. \quad (3)$$

Fractionalized quantum number. The action of an order-two crystal symmetry X on an anyon is fractionalized if acting \tilde{X} *twice* on a *single* anyon yields $\tilde{X}^2 = -1$. To detect such fractionalized quantum number, we act X *once* on an excited state containing *two* anyons, whose positions are *swapped* by X [25]. Specifically, \tilde{X} maps an anyon at a site i to another anyon at the image site $X(i)$ and vice versa.

The symmetry action on an anyon is accompanied by additional gauge transformations [2],

$$\tilde{X}a_i = U_i a_{X(i)}, \quad \tilde{X}a_{X(i)} = U_{X(i)} a_i. \quad (4)$$

Therefore, acting \tilde{X} twice on the anyon a_i leaves anyon at its original position but yields a factor $\tilde{X}^2 a = U_{X(i)} U_i a$.

Alternatively, if one perform the operation X once on a physical wave function $|\Psi\rangle$ that contains a pair of anyons at i and $X(i)$, the same phase factors U_i and $U_{X(i)}$ are collected from each anyon, so that the pair of spinons acquires the same total phase of $U_{X(i)}U_i$. Importantly, if the anyon under consideration is a fermion, there is an additional statistical sign due to the exchange of two fermions under X . To summarize, when a bosonic anyon carries a fractionalized quantum number $\tilde{X}^2 = -1$, the parity eigenvalue of an excited state $|\Psi\rangle$ containing a pair of such anyons is opposite to that of the ground state, from which $|\Psi\rangle$ is created. For fermionic anyons, $\tilde{X}^2 = -1$ implies that the parity eigenvalues of $|\Psi\rangle$ and $|G\rangle$ are identical.

We now show that detecting $\tilde{X}^2 = \pm 1$ for spinons can be further simplified when the spin liquid is constructed from parton methods (using either the Schwinger-boson or Abrikosov-fermion approach), which put exactly one spinon on every lattice site. Specifically, we choose a lattice geometry with $4n + 2$ sites, so that the ground state contains an *odd* number of pairs of spinons. The parity eigenvalue of such a ground state is then equal to the parity of a single pair of spinons, which in turn detects $\tilde{X}^2 = -1$ as described above. Importantly, the contribution to the parity eigenvalue from the fractional quantum number is independent of the topological sector of the ground state, in contrast to the previous case involving the commutation relation between \tilde{X} and \tilde{T}_1 . This will be demonstrated with concrete examples below.

\mathbb{Z}_2 spin liquids on kagome lattices. We now apply our method of detecting crystal symmetry fractionalization to \mathbb{Z}_2 spin liquid states on the kagome lattice. Recent numerical studies of the spin- $\frac{1}{2}$ Heisenberg model on the kagome lattice [5–9] have found strong evidence for a gapped spin liquid state, likely with a \mathbb{Z}_2 topological order (see however, Ref. 26). On the other hand, various types of \mathbb{Z}_2 spin liquids on the kagome lattice that differ in symmetry properties have been theoretically constructed using parton methods in early studies [11–13]. In what follows, we will connect the numerical findings to theoretical constructions and show how to determine which of the \mathbb{Z}_2 spin liquid states theoretically proposed so far is consistent with the ground state of the Heisenberg model on the kagome lattice.

To start, we quickly describe the parton construction of various \mathbb{Z}_2 spin liquid states, paying particular attention to the role of crystal symmetry. Parton constructions postulate that the low-energy dynamics of the spin liquid phase is described by gapped spinons (which carry \mathbb{Z}_2 gauge charge) interacting with \mathbb{Z}_2 gauge fields. Depending on the \mathbb{Z}_2 background flux patterns, the spinon exhibits different crystal symmetry fractionalizations, thus leading to distinct spin liquid states. This is because in the presence of gauge flux, crystal symmetries acting on a spinon involve additional \mathbb{Z}_2 gauge transformations. For example, when there is a π flux within a unit cell, trans-

lations of spinons correspond to the magnetic translation group with the property $\tilde{T}_1\tilde{T}_2 = -\tilde{T}_2\tilde{T}_1$, resulting in a fractionalized commutation relation.

In the parton construction, spin liquids with different \mathbb{Z}_2 background flux patterns are classified using the projective symmetry group (PSG) analysis invented by Wen [2], from which we can derive crystal symmetry fractionalization of bosonic and fermionic spinons. Below we derive the crystal symmetry fractionalization for \mathbb{Z}_2 spin liquids on the kagome lattice that were constructed using the Schwinger-boson approach in previous works [11, 12]. The PSG analysis by Wang and Vishwanath [12] has found that there are four spin liquid states with different \mathbb{Z}_2 flux patterns, which are adiabatically connected to nearest-neighbor resonating-valence-bond states and therefore have better variational energy than other states. Hence we use them as examples to demonstrate our method of detecting crystal symmetry fractionalization. These four states are labeled by three \mathbb{Z}_2 variables (p_1, p_2, p_3) ; for the sake of completeness, this terminology from Ref. 12 is reviewed in Sec. I of the Supplemental Material.

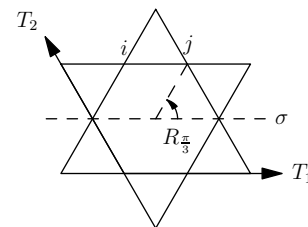


FIG. 1. The definition of crystal symmetry operations. $T_{1,2}$, σ , and $R_{\pi/3}$ label the symmetry operations of translation, mirror reflection, and sixfold rotation, respectively.

The kagome lattice has three independent symmetry operations: $T_{1,2}$, σ , and $R_{\pi/3}$, which denote translation, mirror reflection, and rotation, respectively, and their definition is shown in Fig. 1. A straightforward translation of terminology shows that (p_1, p_2, p_3) in the PSG analysis directly yields the crystal symmetry fractionalizations of the bosonic spinon excitations (denoted by b), listed in the first row of Table I. Here, $\tau_{T_2} = \pm 1$ labels the fractionalization of the commutation relation between T_1 and T_2 , defined by $\tilde{T}_1\tilde{T}_2 = \tau_{T_1}\tilde{T}_2\tilde{T}_1$. Likewise, τ_σ is defined by $\tilde{T}_1\tilde{\sigma} = \tau_\sigma\tilde{T}_1\tilde{\sigma}$, and the fractionalization of commutation relation between T_1 and the twofold rotation $R_\pi \equiv R_{\pi/3}^3$ takes the form of $\tilde{T}_1\tilde{R}_\pi = \tau_{R_\pi}\tilde{R}_\pi\tilde{T}_1^{-1}$. All three τ 's are equal for the four spin liquid states we consider. In addition, quantum number fractionalizations $\tilde{\sigma}^2 = \pm 1$ and $\tilde{R}_{\pi/3}^6 = \pm 1$ are listed in the last two columns of Table II.

A limitation of the previous PSG analysis is that it is tied to the Schwinger-boson formalism and hence only gives the crystal symmetry fractionalization of the bosonic spinons. The vison excitation in all four states has the same crystal symmetry fractionalization [4, 27]:

TABLE I. Crystal symmetry fractionalizations of different anyon excitations. b , f , and v denotes the bosonic spinon, the fermionic spinon and the vison, respectively.

Anyon	$\tau_{T_1}^a = \tau_\sigma^a = \tau_{R_\pi}^a$	$\tilde{\sigma}^2$	$\tilde{R}_{\frac{\pi}{3}}^6 = \tilde{R}_\pi^2$
b	$(-1)^{p_1}$	$(-1)^{p_2}$	$(-1)^{p_1+p_3}$
f	$(-1)^{p_1+1}$	$(-1)^{p_2+1}$	$(-1)^{p_1+p_3+1}$
v	-1	$+1$	$+1$

$\tau_{T_2} = \tau_\sigma = \tau_{R_\pi} = -1$ and $\tilde{\sigma}^2 = \tilde{R}_\pi^2 = 1$. This result can be simply obtained from the charge-flux duality: in a spin liquid state with odd number of spinons per unit cell as is the case for the kagome lattice, the vison always sees a π flux per unit cell because a spinon is a π flux to a vison. As a result, the vison always has the property $\tilde{T}_1\tilde{T}_2 = -\tilde{T}_2\tilde{T}_1$.

We now use the method of flux attachment to derive the crystal symmetry fractionalization for the fermionic spinon, which is equivalent to a composite of a bosonic spinon and a vison—the latter is a π flux to the former. Compared to a bosonic spinon, the fermionic spinon always sees an extra π flux per unit cell due to the vison attached to it; hence $\tau_{T_2}^b = -\tau_{T_2}^f$. Similarly, the difference in \tilde{R}_π^2 between bosonic and fermionic spinons follows from the fact that the attachment of a π flux changes the angular momentum between integer and half-integer values [28]. These results can also be derived using general methods described in Sec I of the Supplemental Material, and are summarized in the second row of Table I [29].

TABLE II. Correspondence between Schwinger-boson and Abrikosov-fermion constructions. p_i labels the PSG solutions of Schwinger-boson construction [12]. The $Q_1 = \pm Q_2$ labels are used by Sachdev [11], and the labels in the last column are used by Lu *et al.* [13].

(p_1, p_2, p_3)	Label in Ref. 11	Label in Ref. 13
$(0, 0, 1)$	$Q_1 = -Q_2$	$Z_2[0, \pi]\alpha$
$(0, 1, 0)$	$Q_1 = Q_2$	$Z_2[0, \pi]\beta$
$(1, 0, 1)$		$Z_2[0, 0]B$
$(1, 1, 0)$		$Z_2[0, 0]A$

As an independent check of the above results, we find that the above four spin liquid states constructed from the Schwinger-boson approach can be equivalently described using the Abrikosov-fermion approach. To establish the mapping between the two parton constructions, we match the ground states of spin liquids in the nearest-neighbor resonating-valence-bond limit, given by the Gutzwiller projection on the corresponding parton

wavefunctions in the two constructions:

$$|\psi\rangle = P_G \exp \left[\sum_{\langle ij \rangle} \xi_{ij} \epsilon_{\alpha\beta} b_{i\alpha}^\dagger b_{j\beta}^\dagger \right] |0\rangle, \quad (5)$$

$$|\psi\rangle = P_G \exp \left[\sum_{\langle ij \rangle} \zeta_{ij} \epsilon_{\alpha\beta} f_{i\alpha}^\dagger f_{j\beta}^\dagger \right] |0\rangle. \quad (6)$$

Here ξ_{ij} and ζ_{ij} are antisymmetric and symmetric scalars on the nearest-neighbor bonds $\langle ij \rangle$ used in Schwinger-boson and Abrikosov-fermion constructions, respectively. The values of ξ_{ij} or ζ_{ij} on bonds of the kagome lattice are given by the corresponding PSG analysis. By equating Eq. (5) and (6), we find explicitly the mapping between ξ_{ij} and ζ_{ij} for each of the four spin liquid states [30, 31]. As a byproduct, this mapping establishes the correspondence between the notation of the Schwinger-boson [11, 12] formalism (p_1, p_2, p_3) with that of the Abrikosov-fermion [13] formalism, as shown in Table II. From this mapping, we have confirmed the results in Table I (see Sec II of the Supplementary Material for details).

TABLE III. Ratios between X -symmetry parity eigenvalues of $|G_a\rangle$ and $|G_1\rangle$. The results depend on the commutation relation fractionalization $\tau_{T_2}^b = -\tau_{T_2}^f = (-1)^{p_1}$, and the ratios are the same for $X = T_2, \tau$ and R_π .

p_1	λ_X^b/λ_X^1	λ_X^v/λ_X^1	λ_X^f/λ_X^1
0	+1	-1	-1
1	-1	-1	+1

Having derived the crystal symmetry fractionalization of anyons for all four spin liquids on the kagome lattice, we can now determine the symmetry representations of the ground states for each spin liquid, by using the general relation between the two as described in the first part of this work. First, based on Eq. (3) and the results of commutation relation fractionalizations summarized in Table I, the ratios between symmetry eigenvalues of different ground states are determined and the results are summarized in Table III.

Second, if all other aspects of the symmetry fractionalization are the same, a difference in the quantum number fractionalization results in a uniform parity change in the symmetry representation of ground states in all topological sectors. This relation can be obtained by explicitly calculating the parity eigenvalues of the model wave functions in Eq. (5) and Eq. (6). The results are summarized in Table III and the details of the derivation is given in Sec. III of the Supplemental Material. These results are determined from projected mean field wave functions but they also apply to general wave functions in the same topologically ordered phase, because the crystal symmetry representations are invariant when

the state is smoothly deformed without breaking crystal symmetries.

TABLE IV. Crystal symmetry representations of ground states in different topological sectors on a torus with odd-by- $(4n+2)$ unit cells. $|G_a\rangle$ denotes the ground state with an anyon flux a in the direction of T_1 , where $a = 1, b, v$, and f denotes the trivial anyon, bosonic spinon, the vison and the fermionic spinon, respectively.

X	$ G_1\rangle$	$ G_b\rangle$	$ G_v\rangle$	$ G_f\rangle$
T_2	1	$(-1)^{p_1}$	-1	$(-1)^{p_1+1}$
σ	$(-1)^{p_2}$	$(-1)^{p_1+p_2}$	$(-1)^{p_2+1}$	$(-1)^{p_1+p_2+1}$
R_π	$(-1)^{p_3}$	$(-1)^{p_1+p_3}$	$(-1)^{p_3+1}$	$(-1)^{p_1+p_3+1}$

Summarizing the above results, we see that the PSG parameters p_2 and p_3 determines the parity eigenvalues of the ground state $|G_1\rangle$, and then using p_1 the parity eigenvalues of the other sectors are also determined. Hence we can obtain from (p_1, p_2, p_3) the crystal symmetry representations of all topological sectors on a torus with odd-by- $(4n+2)$ unit cells, as summarized in Table IV.

Conclusions. In this work we propose a method to detect crystal symmetry fractionalizations from the crystal symmetry representations of the ground states. On a torus with $4n+2$ sites, the ratio between symmetry parity eigenvalues of ground states in different topological sectors detects the fractionalization of commutation relation with a translation symmetry, and a uniform sign change in all sectors detects the quantum number fractionalization.

Our method can be applied to study the nature of the topological order of the \mathbb{Z}_2 spin liquid states obtained in numerical studies. Particularly using the infinite-size density matrix renormalization group (DMRG) method [32] or an infinite projected entangled pair states (PEPS) ansatz [33] the ground states in different topological orders can be obtained on an infinite cylinder and labeled with the anyon type by calculating the modular matrices [32, 34, 35]. To study both commutation relation fractionalization and quantum number fractionalization, we suggest using a cylinder $(4n+2)$ unit cells wide. Then the crystal symmetry fractionalization studied in this work can be determined by putting the system on a torus with a length of an odd number of unit cells and examining the crystal symmetry representation of topologically degenerate ground states. For the \mathbb{Z}_2 spin liquid states discussed above, the results are shown in Table IV.

In this work we explicitly derived the crystal symmetry quantum number of ground states and the fractional symmetry quantum number of anyons for four \mathbb{Z}_2 spin liquid states on the kagome lattice [12]. Our method can be used straightforwardly to study additional spin liquid states that have been theoretically proposed [4, 12, 13].

We thank Lukasz Cincio, Michael Hermele, Yuan-Ming

Lu, Guifre Vidal, Yuan Wan, and Qing-Rui Wang for invaluable discussions. Y.Q. is supported by NSFC Grant No. 11104154. L.F. is supported by the DOE Office of Basic Energy Sciences, Division of Materials Sciences and Engineering, under Award No. DE-SC0010526. This research was supported in part by Perimeter Institute for Theoretical Physics. Research at Perimeter Institute is supported by the Government of Canada through Industry Canada and by the Province of Ontario through the Ministry of Research and Innovation.

Note added. After completing our manuscript we were informed of a related work [36].

-
- [1] R. B. Laughlin, Phys. Rev. Lett. **50**, 1395 (1983).
 - [2] X.-G. Wen, Phys. Rev. B **65**, 165113 (2002).
 - [3] A. M. Essin and M. Hermele, Phys. Rev. B **87**, 104406 (2013).
 - [4] Y.-M. Lu, G. Y. Cho, and A. Vishwanath, arXiv:1403.0575v2.
 - [5] S. Yan, D. A. Huse, and S. R. White, Science **332**, 1173 (2011).
 - [6] T. Tay and O. I. Motrunich, Phys. Rev. B **84**, 020404 (2011).
 - [7] H.-C. Jiang, Z. Wang, and L. Balents, Nat. Phys. **8**, 902 (2012).
 - [8] S. Depenbrock, I. P. McCulloch, and U. Schollwöck, Phys. Rev. Lett. **109**, 067201 (2012).
 - [9] I. Rousochatzakis, Y. Wan, O. Tchernyshyov, and F. Mila, Phys. Rev. B **90**, 100406 (2014).
 - [10] X. Chen, Z.-C. Gu, Z.-X. Liu, and X.-G. Wen, Phys. Rev. B **87**, 155114 (2013).
 - [11] S. Sachdev, Phys. Rev. B **45**, 12377 (1992).
 - [12] F. Wang and A. Vishwanath, Phys. Rev. B **74**, 174423 (2006).
 - [13] Y.-M. Lu, Y. Ran, and P. A. Lee, Phys. Rev. B **83**, 224413 (2011).
 - [14] X.-G. Wen, Phys. Rev. B **44**, 2664 (1991).
 - [15] X.-G. Wen, Int. J. Mod. Phys. B **05**, 1641 (1991).
 - [16] Y.-M. Lu *et al*, Seminar talk at Institut for Advanced Study, Tsinghua University.
 - [17] H. Yao, L. Fu, and X.-L. Qi, arXiv:1012.4470.
 - [18] A. Mesaros and Y. Ran, Phys. Rev. B **87**, 155115 (2013).
 - [19] Y.-M. Lu and A. Vishwanath, arXiv:1302.2634.
 - [20] M. Barkeshli, P. Bonderson, M. Cheng, and Z. Wang, arXiv:1410.4540.
 - [21] A. M. Essin and M. Hermele, Phys. Rev. B **90**, 121102(R) (2014).
 - [22] L. Wang, A. Essin, M. Hermele, and O. Motrunich, arXiv:1409.7013.
 - [23] See Supplemental Material for more technical details of the derivation discussed in the main text.
 - [24] A. Y. Kitaev, Ann. Phys. (N. Y.) **303**, 2 (2003).
 - [25] Here our operational definition of fractionalized quantum number is different from Ref. 4 but our results are consistent. This is detailed in Sec. I of the Supplemental Material.
 - [26] Y. Iqbal, F. Becca, and D. Poilblanc, Phys. Rev. B **84**, 020407(R) (2011).
 - [27] Y. Huh, M. Punk, and S. Sachdev, Phys. Rev. B **84**,

- 094419 (2011).
- [28] F. Wilczek, Phys. Rev. Lett. **48**, 1144 (1982).
 - [29] After completing this work we learnt that identical results have been obtained in the updated version of Ref. 4.
 - [30] S. Yunoki and S. Sorella, Phys. Rev. B **74**, 014408 (2006).
 - [31] F. Yang and H. Yao, Phys. Rev. Lett. **109**, 147209 (2012).
 - [32] B. Bauer, L. Cincio, B. P. Keller, M. Dolfi, G. Vidal, S. Trebst, and A. W. W. Ludwig, Nat. Commun. **5**, 5137 (2014).
 - [33] J. Jordan, R. Orús, G. Vidal, F. Verstraete, and J. I. Cirac, Phys. Rev. Lett. **101**, 250602 (2008).
 - [34] Y. Zhang, T. Grover, A. Turner, M. Oshikawa, and A. Vishwanath, Phys. Rev. B **85**, 235151 (2012).
 - [35] L. Cincio and G. Vidal, Phys. Rev. Lett. **110**, 067208 (2013).
 - [36] M. Zaletel, Y.-M. Lu, and A. Vishwanath, arXiv:1501.01395.
-

Supplemental Material

In this supplemental material we provide some technical details of the derivations outlined in the main text.

I. CRYSTAL SYMMETRY FRACTIONALIZATIONS OF BOSONIC AND FERMIONIC SPINONS.

In this section we derive the relation between crystal symmetry fractionalizations of bosonic and fermionic spinons. In a Z_2 spin liquid states, both of the three types of topological excitations (bosonic spinon, fermionic spinon and vison) carry projective representations of the crystal symmetry group, and different anyon carries a projective representation with different crystal symmetry fractionalizations. However, the crystal symmetry fractionalizations of different anyons are not independent, and particularly the symmetry fractionalization of fermionic spinon can be derived from the ones of the bosonic spinon and vison, as the former is a bound state of the latter [1]. For Z_2 spin liquids with odd number of spinons per unit cell, the symmetry fractionalization of the vison is fixed [2, 3]. Therefore the symmetry fractionalization of the fermionic spinon can be uniquely determined from the one of the bosonic spinon. In this section we focus on the following three crystal symmetry fractionalizations on the kagome lattice: the commutation relation fractionalization between T_1 and T_2 , and the quantum number fractionalization of σ^2 and R_π^2 . These results are used in the main text to obtain Table I.

Firstly, the fractionalization of commutation relation between T_1 and T_2 of fermion, $\tau_{T_2}^f$, can be derived from the corresponding fractionalizations of the bosonic spinon and of the vison [1],

$$\tau_{T_2}^f = \tau_{T_2}^b \tau_{T_2}^v. \quad (1)$$

For Z_2 spin liquids with odd number of spinons per unit cell, $\tau_{T_2}^v = -1$ [2]. Hence we always have $\tau_{T_2}^f = -\tau_{T_2}^b$ [3]. As explained in the main text this can be understood intuitively using flux attachment.

Next, we consider the reflection symmetry σ . We find as a bound state of a bosonic spinon and a vison, the fractionalized quantum number of a fermion is the product of the

quantum numbers of a bosonic spinon and that of a vison, times an additional twist factor $t = -1$

$$\tilde{\sigma}_f^2 = -\tilde{\sigma}_b^2\tilde{\sigma}_v^2, \quad (2)$$

where $\tilde{\sigma}_a$ denotes the projective representation of σ acting on anyon type a . The twist factor $t = -1$ can be calculated by examining the reflection parity eigenvalue of a wave function $|\Psi\rangle$ containing two fermionic spinon excitations located at two sites related by σ . As discussed in the main text, if $\tilde{\sigma}_f^2 = +1$, the reflection parity eigenvalues of $|\Psi\rangle$ and of the ground state $|G\rangle$ are opposite because of the Fermi statistical sign of exchanging two fermions, and if $\tilde{\sigma}_f^2 = -1$ the two eigenvalues are the same. On the other hand, $|\Psi\rangle$ can also be viewed as a wave function containing two bosonic spinons and two visons. Therefore the ratio between reflection parity eigenvalues of $|\Psi\rangle$ and of $|G\rangle$ is also given by $\tilde{\sigma}_b^2\tilde{\sigma}_v^2$. Comparing these two results we conclude that the twist factor $t = -1$ in Eq. (2). For the Z_2 spin liquid states we consider, the vison always has $\tilde{\sigma}_b^2 = +1$ [2]. Hence the fermionic spinon and bosonic spinon always have opposite reflection quantum number fractionalization $\tilde{\sigma}_f^2 = -\tilde{\sigma}_b^2$.

Our conclusion of $t = -1$ should be contrasted with the incorrect result of the twist factor obtained in Ref. 1. We note that the phase of the two-fermion wave function depends on the ordering of the two fermions, and after mirror reflection the exchange of the two fermions gives the Fermi statistical sign of -1 . This minus sign is the key in the above derivation of $t = -1$. As an independent check, in Sec. II we explicitly derive the mapping between Schwinger-boson and Abrikosov-fermion constructions, which gives the same mapping between the crystal symmetry fractionalizations of the bosonic and fermionic spinons.

We also note that a different operational definition was used by Lu *et al.* [3], which lead to the identical result. In their definition they considered two anyons, whose positions are *unchanged* under mirror reflection, in contrast to our definition where the position of the anyons are *exchanged* by mirror reflection. Their definition is more involved to study when the translation operator (which connects the two positions of the anyons) does not commute with the reflection.

Similarly for the inversion symmetry the twist factor t is also -1 because of the Fermi statistical sign, so $\tilde{R}_{\pi,f}^2 = -\tilde{R}_{\pi,b}^2\tilde{R}_{\pi,v}^2$. Again for the Z_2 spin liquids on the kagome lattice we always have $\tilde{R}_{\pi,v}^2 = +1$. This twist factor $t = -1$ was also obtained using different methods by Essin and Hermele [1]. Therefore the fermionic spinon and bosonic spinon have opposite inversion quantum number fractionalization $\tilde{R}_{\pi,f}^2 = -\tilde{R}_{\pi,b}^2$.

II. ABRIKOSOV-FERMION REPRESENTATION OF SCHWINGER-BOSON SPIN LIQUID STATES

In this section we discuss the Abrikosov-fermion representation of the nearest-neighbor Schwinger-boson spin liquid states. In general these two ways of constructing spin liquid states can describe several common Z_2 spin liquid states [3], and particularly spin liquid states with pairings on nearest-neighbor bonds only can be described by both of the two constructions [4, 5].

We begin with a brief review of the four bosonic PSG solutions discussed in the main text, which were studied in details by Wang and Vishwanath [6]. These four PSG solutions are labeled by three Z_2 variables (p_1, p_2, p_3) , which parameterizes the projective crystal symmetry representation carried by the bosonic spinon operators,

$$\phi_{T_1}(\mathbf{r}) = 0, \quad (3a)$$

$$\phi_{T_2}(\mathbf{r}) = p_1 \pi r_1, \quad (3b)$$

$$\phi_{\sigma}(\mathbf{r}) = p_2 \frac{\pi}{2} + p_1 \pi r_1 r_2, \quad (3c)$$

$$\phi_{\frac{\pi}{3}}(\mathbf{r}) = p_3 \frac{\pi}{2} + p_1 \pi \frac{r_2(r_2 - 1 + 2r_1)}{2}. \quad (3d)$$

where $\phi_X(\mathbf{r})$ denotes the additional $U(1)$ phase acquired by the bosonic operator after the symmetry operation X . In other words, the projective symmetry representation of X carried by $b_{i\alpha}$ is

$$X : b_{i\alpha} \rightarrow e^{i\phi_X(\mathbf{r}_i)} b_{X(i)\alpha}. \quad (4)$$

The PSG solution in Eq. (3) determines both the crystal symmetry fractionalization of the bosonic spinon and the pattern of ξ_{ij} in the mean field wave function in Eq. (6) of the main text. On one hand, the PSG solution describes the projective representation of the crystal symmetry group carried by the bosonic spinons, and from it their crystal symmetry fractionalization listed in Table I can be derived. On the other hand, it also describes the pattern of ξ_{ij} such that the wave function in Eq. (6) is invariant under symmetry transformations. The patterns of ξ_{ij} for the four different PSG solutions are plotted in Fig. 1, where on each bond the value of $\xi_{ij} = \pm 1$ is represented by an arrow because $\xi_{ij} = -\xi_{ji}$. These patterns are the same as the patterns of the nearest-neighbour pairing terms listed in Ref. 6.

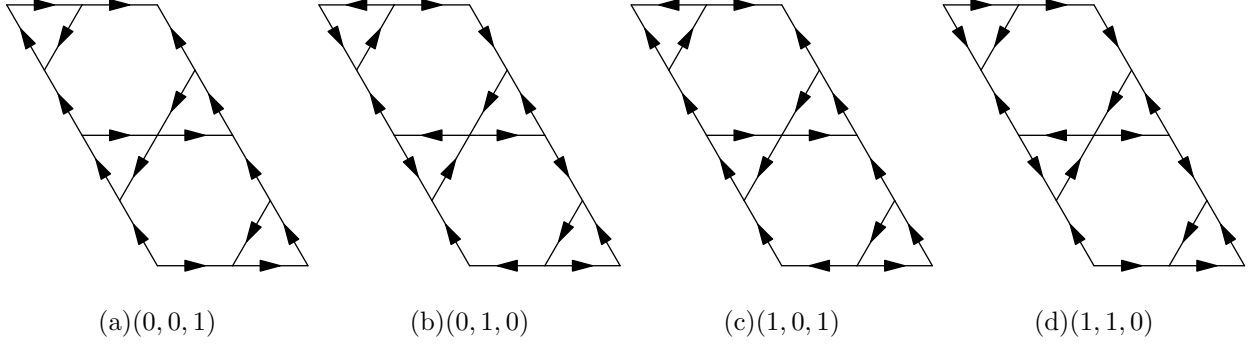


FIG. 1. Pairing amplitude ξ_{ij} of Schwinger-boson mean field constructions with four different PSG solutions. The arrows represent the value of $\xi_{ij} = \pm 1$, where an arrow from i to j indicates $\xi_{ij} = -\xi_{ji} = +1$.

TABLE I. Summary of PSG solutions for the Schwinger-boson and Abrikosov-fermion construction of the four Z_2 spin liquid state.

(p_1^b, p_2^b, p_3^b)	(p_1^f, p_2^f, p_3^f)
(1, 1, 0)	(0, 0, 0)
(0, 1, 0)	(1, 0, 0)
(1, 0, 1)	(0, 1, 1)
(0, 0, 1)	(1, 1, 1)

Starting from a specific Schwinger-boson PSG solution, we derive the PSG solution of the corresponding Abrikosov-fermion PSG by first working out the pattern of ζ_{ij} using the correspondence between ξ_{ij} and ζ_{ij} given by Ref. 5, and then identify the compatible

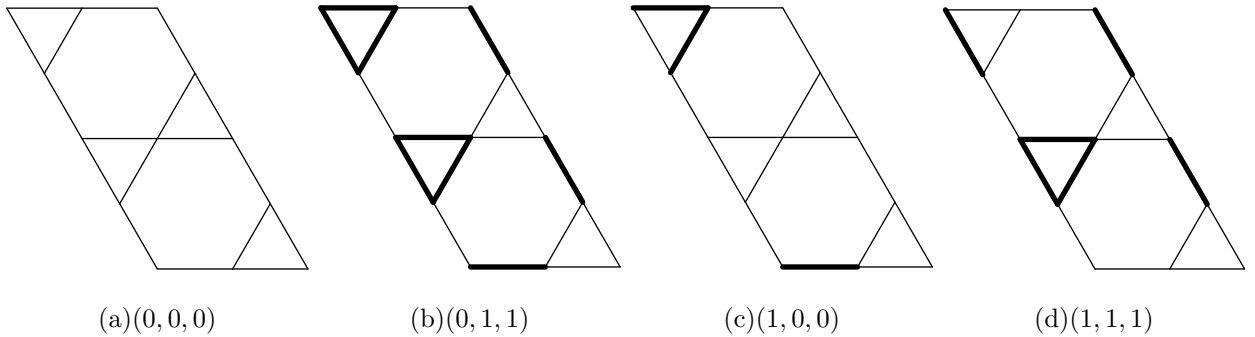


FIG. 2. Pairing amplitude ζ_{ij} of Abrikosov-fermion mean field constructions with four different PSG solutions. A thin (thick) bond represents $\zeta_{ij} = +1$ (-1), respectively.

PSG solutions, which are described by the other four combinations of (p_1, p_2, p_3) that does not describe a nearest-neighbor Schwinger-boson ansatz. These Abrikosov-fermion PSG solutions are a subset of the ones given by the general classification in Ref. 7. Here we denote the PSG parameters of the Schwinger-boson and Abrikosov-fermion ansatz by p_i^b and p_i^f , respectively. For each Schwinger-boson state labeled by (p_1^b, p_2^b, p_3^b) , the corresponding Abrikosov-fermion PSG solution (p_1^f, p_2^f, p_3^f) and the label as used in Ref. 7 is listed in Table I.

In these four Abrikosov-fermion PSG solutions, the fermionic spinons transform under crystal symmetry operations with an additional U(1) phase described by Eq. (3), and these solutions are a subset of the possible PSG solutions, with the general SU(2) gauge transformations restricted to the U(1) subgroup. Hence these four states are included in the general classification given by Lu *et al.* [7]. We can label these states with the notation used in Ref. 7 by calculating the topological invariants of symmetry fractionalizations listed in Ref. 3.

TABLE II. Summary of PSG solutions and exactly solvable Hamiltonians of the four different Z_2 state realizable in the quantum dimer model.

Symmetry fractionalizations	(p_1^f, p_2^f, p_3^f)	SU(2) PSG
$T_2^{-1}T_1^{-1}T_2T_1$	$(-1)^{p_1^f}$	η_{12}
σ^2	$(-1)^{p_2^f}$	$\eta_\sigma \eta_{\sigma C_6}$
$(R_{\frac{\pi}{3}}\sigma)^2$	$(-1)^{p_2^f + p_3^f}$	η_σ
$(R_{\frac{\pi}{3}})^6$	$(-1)^{p_1^f + p_3^f}$	η_{C_6}
$\sigma^{-1}T^{-1}\sigma T$	$(-1)^{p_2^f}$	$\eta_{\sigma T} \eta_{C_6 T}$
$R_{\frac{\pi}{3}}^{-1}T^{-1}R_{\frac{\pi}{3}}T$	$(-1)^{p_3^f}$	$\eta_{C_6 T}$

TABLE III. Summary of PSG solutions and exactly solvable Hamiltonians of the four different Z_2 state realizable in the quantum dimer model.

(p_1^f, p_2^f, p_3^f)	η_{12}	η_σ	$\eta_{\sigma T}$	$\eta_{\sigma C_6}$	$\eta_{C_6 T}$	η_{C_6}	SU(2) PSG Label
(0, 0, 0)	+1	+1	+1	+1	+1	+1	$Z_2[0, 0]A$
(1, 0, 0)	-1	+1	+1	+1	+1	-1	$Z_2[0, \pi]\beta$
(0, 1, 1)	+1	+1	+1	-1	-1	-1	$Z_2[0, 0]B$
(1, 1, 1)	-1	+1	+1	-1	-1	+1	$Z_2[0, \pi]\alpha$

Using the PSG solutions in Eq. (3), six symmetry fractionalization invariants are calcu-

lated and listed in Table II. These results are then compared to the same invariants expressed using the Z_2 labels η_A for generic SU(2) PSG solutions[3, 7]. Using these relations we can calculate the labels η_A for the four PSG solutions labeled by p_i^f and the results are listed in Table III. Finally these states can be labeled by the notations defined by Lu *et al.* [7] by comparing the results of η_A to Table III in Ref. 3, and these labels are listed in the last column of Table III.

In summary, starting from a nearest-neighbor pairing Schwinger-boson state with a certain PSG solution, we can first derive the corresponding fermionic PSG solution labeled by (p_1^f, p_2^f, p_3^f) using the mapping in Table I, then label the PSG solution using the notation in Ref 7 using the mapping in Table III. These results are presented in Table II in the main text.

III. PARITY EIGENVALUES OF THE GROUND STATE WAVE FUNCTIONS.

In this section we calculate the σ and R_π parity eigenvalues of the ground state wave functions, which is used to detect the fractionalized quantum numbers of $\tilde{\sigma}^2$ and \tilde{R}_π^2 , as explained in the main text. We first obtain the results using the model wave functions in Eq. (6) and Eq. (7) in the main text, then argue that this result also applies to generic wave functions that belong to the same SET phase.

Here we put our system on a torus with $4n + 2$ sites, so there must be an odd number of unit cells along one direction, and as shown in Table III in the main text different ground states have different parity eigenvalues of σ and R_π . Hence we also need to determine the topological sector the mean field wave functions belong to. Using the sign structure in the mean field wave functions one can show that [8] the Schwinger-boson wave function in Eq. (6) in the main text is a superposition of $|G_1\rangle$ and $|G_b\rangle$, while the Abrikosov-fermion wave function in Eq. (7) in the main text is a superposition of $|G_v\rangle$ and $|G_b\rangle$. Using this result it is easy to identify the ground state crystal symmetry representations from the projected mean field wave functions.

For the two states with $p_1^b = 0$, the crystal symmetry representations can be determined using the Schwinger-boson wave function. In this case their PSG solutions in Eq. (3) are simplified to that after the action of σ or R_π the spinon operator $b_{i\alpha}$ acquires a phase of $p_2^b \frac{\pi}{2}$ and $p_3^b \frac{\pi}{2}$, respectively [6]. Therefore the wave function, containing $4n + 2$ spinons after

the Gutzwiller projection, acquires a phase of $p_2^b\pi$ and $p_3^b\pi$, respectively. Since this wave function is a superposition of $|G_1\rangle$ and $|G_b\rangle$, we conclude that their parity eigenvalues under σ and R_π is $(-1)^{p_2^b}$ and $(-1)^{p_3^b}$, respectively.

For the two states with $p_1^b = 1$, we need to use the Abrikosov-fermion wave function. (In this case the Schwinger-boson wave function is not symmetric because it is a superposition of $|G_1\rangle$ and $|G_b\rangle$, which has different crystal symmetry representations in this certain geometry according to Table III in the main text.) Similarly in these two states the PSG solutions also simplifies to that after the action of σ or R_π the spinon operator $f_{i\alpha}$ acquires a phase of $p_2^f\frac{\pi}{2}$ and $p_3^f\frac{\pi}{2}$, respectively. However in this case in addition to this phase from each spinon, there is an additional sign from the reordering of fermion operators in the Gutzwiller projection operator after the symmetry transformation, which is worked out in Sec. IV. Combining these two phase factors we conclude that the parity eigenvalues of the Abrikosov-fermion wave function, which is a superposition of $|G_v\rangle$ and $|G_b\rangle$, is $(-1)^{p_2^f} = (-1)^{p_2^b+1}$ and $(-1)^{p_3^f+1} = (-1)^{p_3^b+1}$ under σ and R_π , respectively (we used the mapping between p_i^b and p_i^f in Table I). Hence according to the results in Table III in the main text the parity eigenvalues of $|G_1\rangle$ are $(-1)^{p_2^b}$ and $(-1)^{p_3^b}$.

IV. FERMION REORDERING SIGNS.

In this section we compute the fermion operator reordering signs that appears in the definition of the Gutzwiller projection operator for the Abrikosov-fermion mean field state in Eq. (7) in the main text. The projection operator P_G contain a product of fermion operators on each lattice sites, and after a crystal symmetry transformation the ordering of the sites is changed, so the aforementioned wave function can acquire an additional minus sign due to the reordering of fermion operators. This sign ϕ_X^f , where X denotes the crystal symmetry operation, is computed here, for a system with $4n + 2$ sites.

For the translation symmetry operation T_1 , we can order the fermion operators first from left to right in each row in the direction of T_1 , then from top to bottom for each row in the direction of T_2 . After translation, in each row we need to move one fermion operator from the beginning to the end. Assuming there are n_1 and n_2 unit cells in the direction of T_1 and T_2 , respectively, the reordering of the fermion operators gives a sign of $(-1)^{n_1+1}$ for each row, and a total sign of $(-1)^{n_2(n_1+1)} = (-1)^{n_2}$ because the total number of unit cells n_1n_2

is odd. Since we have an odd number of sites per unit cell and each sublattice is giving the same contribution, the total phase is $\varphi_{T_1}^f = n_2\pi$. Similarly we have $\varphi_{T_2}^f = n_1\pi$. Note that since $n_1n_2 = 4n + 2$, one of these two factors is π and the other is zero.

For the inversion symmetry operation R_π , we can order the fermion operators in a way that the two sites related by R_π appear together:

$$|\psi\rangle_p = \left(f_{i_1}^\dagger f_{i'_1}^\dagger\right) \left(f_{i_2}^\dagger f_{i'_2}^\dagger\right) \cdots \left(f_{i_{6n+3}}^\dagger f_{i'_{6n+3}}^\dagger\right) |0\rangle, \quad (5)$$

where $f_i^\dagger = \sum_a f_{ia}^\dagger$, and i_l^\dagger labels the lattice site that is related by R_π to site i . Since there are in total $4n + 2$ unit cells in the system, there are in total $6n + 3$ pairs of sites. After the operation of R_π , we need to exchange the two fermion operators within each pair to restore the fermion order, and each pair contributes a minus sign. Since the total number of pairs is odd, we conclude $\varphi_{R_\pi}^f = \pi$.

For the mirror reflection symmetry σ , we also order the fermions such that two sites related by σ appear together. However, as shown in Fig. 1 in the main text, there are also sites that are cut by the mirror plane and stays invariant under mirror reflection, and we put them in the beginning of the product, as the following,

$$|\psi\rangle_p = f_{j_1}^\dagger \cdots f_{j_p}^\dagger \left(f_{i_1}^\dagger f_{i'_1}^\dagger\right) \left(f_{i_2}^\dagger f_{i'_2}^\dagger\right) \cdots \left(f_{i_q}^\dagger f_{i'_q}^\dagger\right) |0\rangle, \quad (6)$$

where j_1, \dots, j_p denotes the sites that are on the mirror axis σ . The total number of such sites p equals to the number of unit cells along the direction of σ . In our setup, the number of sites on the mirror plane σ always equal to two modular four. Hence the number of pairs q in Eq. (6) must be an even number. Similar to the previous discussion we conclude $\varphi_\sigma^f = 0$.

-
- [1] A. Essin and M. Hermele, Phys. Rev. B **87**, 104406 (2013).
 - [2] Y. Huh, M. Punk, and S. Sachdev, Phys. Rev. B **84**, 094419 (2011).
 - [3] Y.-M. Lu, G. Y. Cho, and A. Vishwanath, arXiv:1403.0575v2.
 - [4] S. Yunoki and S. Sorella, Phys. Rev. B **74**, 014408 (2006).
 - [5] F. Yang and H. Yao, Phys. Rev. Lett. **109**, 147209 (2012).
 - [6] F. Wang and A. Vishwanath, Phys. Rev. B **74**, 174423 (2006).
 - [7] Y.-M. Lu, Y. Ran, and P. A. Lee, Phys. Rev. B **83**, 224413 (2011).
 - [8] Y. Qi and L. Fu, Unpublished.